Tutor/s

Dr. Arnald Grabulosa Rodríguez
Dept. de Química Inorgànica i Orgànica
Secció de Química Inorgànica

Grau de Química

Treball Final de Grau

Asymmetric olefin hydrogenation with Rh complexes with unsymmetrical diphosphorus ligands.

Hidrogenació asimètrica d'olefines amb complexos de Rh amb lligands difosforats no simètrics.

Javier Eusamio Rodríguez

June 2020

UNIVERSITAT DE BARCELONA

B:KC Barcelona Knowledge Campus
Campus d'Excel·lència Internacional

«...el Sistema Periòdic de Mendelejev [...] era una poesia, més alta i més solemne que totes les poesies digerides a l'escola: pensant-hi bé, tenia rimes i tot!»

Primo Levi, *El Sistema Periòdic*
(traducció de Xavier Riu)

Escriure uns agraïments en les condicions en què s'ha desenvolupat aquest TFG és estrany: no hi ha hagut companys de laboratori amb qui compartir les estones de feina, ni he pogut passar les hores d'oci amb els meus amics xerrant a l'atri. El confinament, sens dubte, ha reduït molt aquesta part més humana que tenen tots els treballs acadèmics i que sempre acaben cristal·litzant en els Agraïments. No obstant això, encara en tinc alguns a fer.

En primer lloc (i l'ordre no és casual), vull agrair al Dr. Arnald Grabulosa tot l'interès i dedicació que ha posat en la seva tasca com a tutor del TFG. Els seus coneixements, la seva atenció a tots els detalls i els seus comentaris han estat molt valuosos i han contribuït a aconseguir que em senti orgullós del resultat final d'aquesta memòria.

En segon lloc, vull agrair la seva existència a la Base de Dades de l'Arnald, que hauria d'ésser considerada com a entitat pròpia (així, en majúscules i tot) i que va avançant lentament però inexorable fins a abastar tots els *papers* de Química mai escrits. Realment m'ha estat una eina molt útil en la realització d'aquest treball.

Com he dit al començament, és una llàstima que aquests Agraïments no puguin allargar-se més, però confio a fer-ho en futurs projectes d'investigació que, essent una mica més afortunats, puguin desenvolupar-se en condicions normals.

REPORT

CONTENTS

1. SUMMARY

In this project, rhodium(I) complexes **C1**–**C3** bearing ligands **L1**–**L3** were intended to be used in the asymmetric hydrogenation of substrates **S1**–**S12**. Complexes **C1** and **C2**, of the type [Rh(COD)(**L**)]BF_4, were prepared in a previous project, while complex **C3** was prepared from ligand **L3**. Ligand **L3** has been synthesized from methylphosphine–borane **P3** and fully characterized, while complex **C3** could only be partially characterized due to the covid19

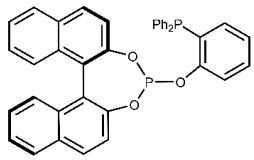

L1

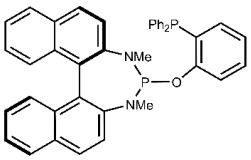

L2

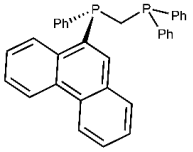

L3

pandemic.

It has been observed that **C3** is a bischelated complex that tends to oxidize in solution. In the future, the synthesis of **C3** will be repeated under stricter inert atmosphere.

Also due to the confinement against covid19, the hydrogenation of substrates **S1**–**S12** has not been possible, and instead a literature search of hydrogenation results with similar ligands has been made.

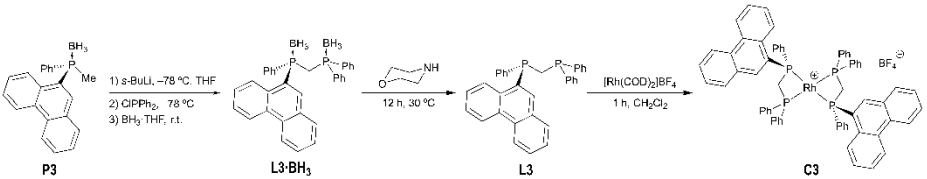

P3 **L3·BH_3** **L3** **C3**

Keywords: asymmetric hydrogenation, Rh, phosphine–phosphite, methylene bridge phosphines.

2. RESUM

En aquest projecte, els complexos de rodi(I) **C1**–**C3** amb els lligands **L1**–**L3** havien de ser emprats en les hidrogenacions asimètriques dels substrats **S1**–**S12**. Els complexos **C1** i **C2**, del tipus [Rh(COD)(**L**)]BF_4, havien estat preparats en un projecte previ, mentre que el complex **C3** ha estat preparat a partir del lligand **L3**. El lligand **L3** ha estat sintetitzat a partir del metilfosfina–borà **P3** i ha estat totalment caracteritzat, mentre que el complex **C3** només ha pogut ser caracteritzat parcialment a causa de la pandèmia del covid19.

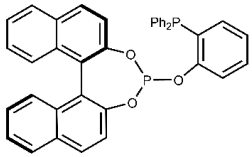

L1

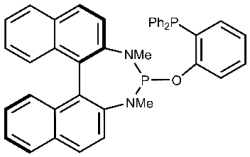

L2

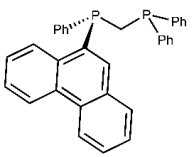

L3

S'ha observat que **C3** és un complex bisquelat que tendeix a oxidar-se en solució. En el futur, es repetirà la síntesi d'aquest complex en una atmosfera inerta més estricta.

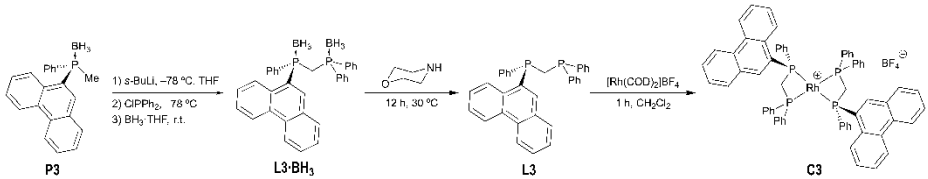

P3 **L3·BH_3** **L3** **C3**

A causa també del confinament pel covid19, la hidrogenació dels substrats **S1**–**S12** no ha estat possible, i en comptes d'això s'ha fet una cerca de bibliografia d'hidrogenacions amb lligands similars.

Paraules clau: hidrogenació asimètrica, Rh, fosfina–fosfit, fosfines amb pont metilè.

3. INTRODUCTION

Catalytic asymmetric hydrogenation is a topic of the utmost importance in current chemistry, as its objective —the obtention of enantiopure products in an efficient (100% atom economy) and environmentally friendly way— is amongst the highest priorities of the pharmaceutical and the agrochemical industries. In these sectors, the optical isomerism of a substance is not a trivial issue, as commonly —due to the ubiquitous presence of chiral compounds in our own cells and in nature in general— one enantiomer can prove to be highly effective while its counterpart is inactive or, in the worst and most extreme cases, even harmful, as it happened with the tragically well-known case of Thalidomide[1]. Thus, the development of efficient synthetic methods of enantiomerically pure compounds is an ever-pursued goal of the greatest importance. Proof of this is the fact that in 2001 the Nobel Prize in Chemistry was awarded to Ryoji Noyori and William S. Knowles "for their work on chirally catalyzed hydrogenation reactions". An important part of Noyori's research focused on the atropoisomeric BINAP ligand, a derivative of which is used in the ligands **L1** and **L2** presented here. On the other hand, Knowles developed DIPAMP, a *P*–stereogenic diphosphine that was implemented in the industrial synthesis of L-DOPA, a drug for Parkinson's disease, showing the industrial applicability of these compounds[2] (Figure 1).

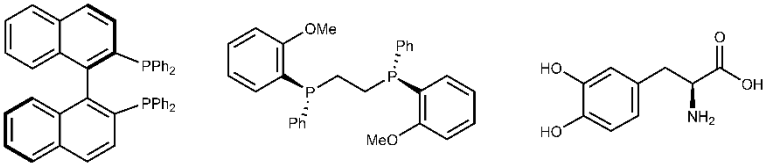

(R)-BINAP *(R,R)*-DIPAMP L-DOPA

Figure 1

In this PROJECT, the focus was to be put on the hydrogenation of twelve different unsaturated substrates (**S1**–**S12**) with three different rhodium(I) complexes (**C1**–**C3**) bearing C_1-symmetric diphosphorus ligands (**L1**–**L3**). **L1** and **L2** are a phosphine–phosphite and phosphine–diamidophosphite ligands (**P–O'P**) respectively, with a phenylene backbone; and **L3** is a single–atom bridged *P*-stereogenic diphosphine. Due to the covid19 confinement, the hydrogenation of

the substrates has been impossible, and instead a literature research of the previously reported hydrogenations of these same substrates has been done.

3.1. SUBSTRATES

Hydrogenation substrates **S1**–**S12** are presented in Figure 2. They are all functionalized olefins[3] and ketimines, but belong to different compound families and exhibit different behaviors

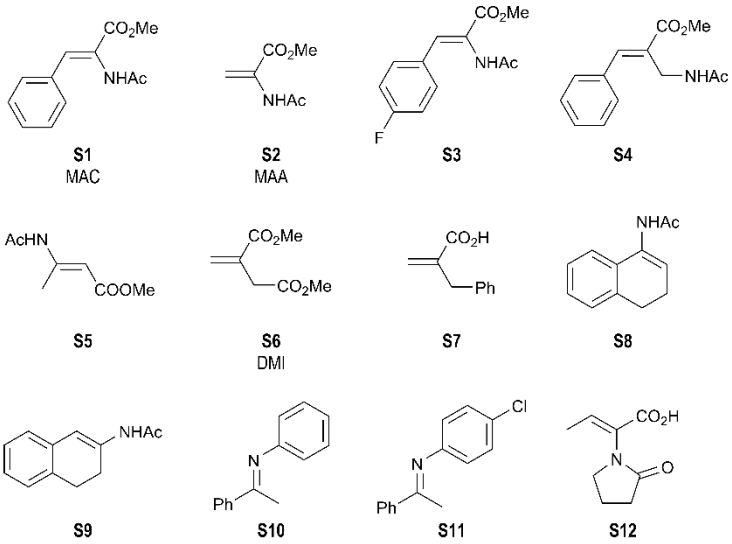

Figure 2: List of substrates hydrogenated in this work.

in hydrogenation. They have been selected for several reasons: for being model substrates in asymmetric hydrogenation of functionalized olefins, for being interesting from the pharmacological perspective and/or for being notoriously difficult to hydrogenate in high enantioselectivity.

3.1.1. (Acetamido)dehydroamino acids

S1–**S5** are usually known as (acetamido)dehydroamino acids, a family of compounds of pharmaceutical relevance, as they offer the possibility of obtaining enantiomerically pure amino acids[4], which are the precursors of many drugs.

In addition, **S1** and **S2** (methyl (*Z*)-α-acetamidocinnamate (MAC) and ethyl α-acetamidoacrylate (MAA), respectively) are α-dehydroamino acids that have been historically used as hydrogenation model substrates alongside with **S6** (DMI). This implies that results of their

hydrogenation will be very comparable with many other studies that used similar ligands[4-8]. **S3** is a *p*-fluorinated derivative of **S1** whose hydrogenation is harder due to its electron-withdrawing fluorine[9]. This family does not only have a use as benchmark substrates, but it also has a presence in many pharmaceutical compounds, like L-azatyrosine (Figure 3), used to treat cancer, which has been synthesized using Rh-catalyzed hydrogenation with the ligand DUPHOS[10].

On the other hand, **S4** and **S5** are β-dehydroaminoacids, a very important family of compounds since they are building blocks in the syntheses of more complex pharmaceutical compounds, including β-peptides or β-lactam antibiotics[11]. Some of these compounds are commercially available and are prescribed, like in the case of sitagliptin or imagabalin hydrochloride (Figure 3), which are used to treat diabetes and anxiety, respectively[12]. Albeit less studied than **S1** and **S2**, the hydrogenation of these substrates can be found in the literature[11, 13].

3.1.2. Itaconic acid derivatives

S6 and **S7** are itaconates, derivatives of itaconic acid. The best known is **S6**, as already mentioned in the above section, due to its role as a benchmark substrate in hydrogenation. It is commonly abbreviated as **DMI**, dimethyl itaconate. Aside the interest of DMI as a model substrate, itaconates are also of crucial importance in many industries, besides from the pharmaceutical one, like the agrochemical or the flavor and fragrance sectors[4]. In the former, some commercially available compounds can be found, like pregabalin (Figure 3), a drug used to epilepsy, anxiety, and other disorders[12].

S7 is a more uncommon itaconate that has its interest in its lack of a second carboxylate group like in **S6**, which makes the enantioselective hydrogenation particularly complicated. Consequently, a catalyst being able to hydrogenate **S7** with good enantioselectivity would be very valuable.

3.1.3. Cyclic enamides

S8 and **S9** are cyclic enamides. Along with **S7**, cyclic enamides pose an interest due to the challenging aspect of their structure: the fact that they have an α-alkyl substituent instead of an electron-withdrawing group (like **S1**–**S3**) complicates the formation of the chelated complex–substrate adduct necessary according to the standard hydrogenation mechanism. Instead, the β-aryl substituent might influence towards the formation of a different chelate that would render the

opposite enantiomer, damaging the enantioselectivity of the catalysis[14]. Moreover, the sterically bulky structure of the enamide further hampers its reactivity with the complex. Thus, enamides have been the subject of some recent hydrogenation studies[6, 8, 15].

Apart from the purely academical interest that enamides have due to its challenging nature, the asymmetric hydrogenation of these compounds is also a well-sought objective for the industry, as enamides too constitute important components of pharmaceutical compounds. One example is cinacalcet (Figure 3), used to treat hyperparathyroidism. One of the steps of its synthesis is the asymmetric hydrogenation of an enamide, which has been carried out with Rh complexes with different phosphine ligands, all of which provided very good results[12, 16].

3.1.4. Ketimines

S10 and **S11** are ketimines, a name given for acyclic imines. They contain the same structure with a small variation: a *p*-chloro group in **S11**, in a similar fashion as **S3** compared to **S1**. The purpose they follow is the same, as well: introducing an electron-withdrawing group to make the hydrogenation more difficult and thus better test the catalyst.

Ketimines are an interesting group of compounds because of how scarcely studied they have been as hydrogenation substrates[17]. They have been found to be difficult substrates because, among other reasons, their hydrogenation products are amines, which have a tendency to coordinate and thus deactivate the catalyst[18].

3.1.5. Levetiracetam precursor

S12 falls somewhat apart from the other substrates considered because it represents a particular case. **S12** is a direct precursor of levetiracetam[12] (Figure 3), an anti-epileptic drug. In order to synthesize the pharmacologically active compound, the (*S*) enantiomer should be obtained.

The hydrogenation of such a compound puts into perspective the importance of these catalysts and their potentially direct application in industrial pharmaceutical processes.

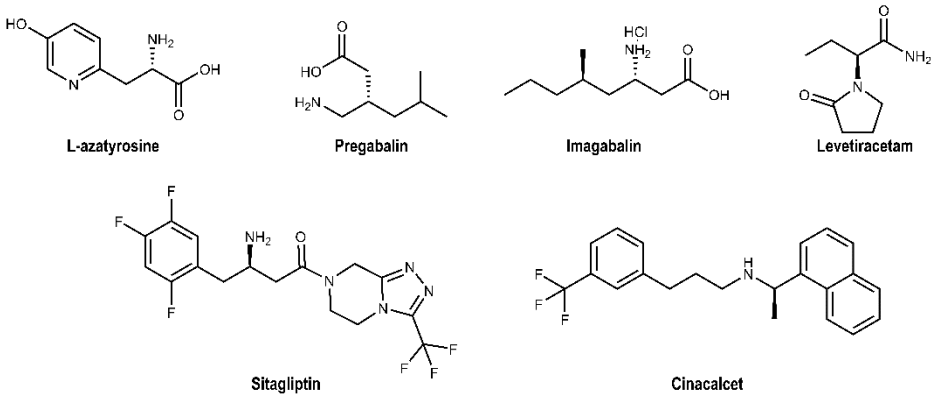

Figure 3: Some pharmaceutically active compounds that have been obtained via asymmetric hydrogenation with Rh compounds.

3.2. COMPLEXES

In this project, attention will be focused on rhodium(I) catalytic precursors bearing diphosphorus ligands. Rh(I) complexes have been used for decades as catalysts because of their electronically favorable properties that allow them to stabilize a wide variety of ligands —from π-donating systems, like alkenes, to σ-donors, like hydrides or phosphines, or π-acceptors, like phosphites— in Rh (I) and Rh(III) oxidation states. Indeed, Rh(III) octahedral complexes are formed after an oxidative addition of dihydrogen to Rh(I) in the hydrogenation mechanism[19].

Through this project, two types of Rh precursors with C_1-symmetric (i.e. the two phosphorus moieties are different) ligands will be evaluated: phosphine-phosphite ligands (**P–OP'**) and a diphosphine (**P–P'**) with a methylene bridge. In total, three ligands will be assessed, **L1**–**L3**.

3.2.1. Complexes with P-OP' ligands

Complexes **C1** and **C2** bear a phosphite-phosphine and a diamidophosphite-phosphine ligand, respectively. A phosphite consists of a P atom bound to three O atoms, while a diamidophosphite contains two amino groups and an O atom, as can be seen in Figure 4. Both of them contain a 1,1'-binaphthyl moiety —as in the previously mentioned BINAP— which presents atropoisomerism and confers the chirality to the ligand.

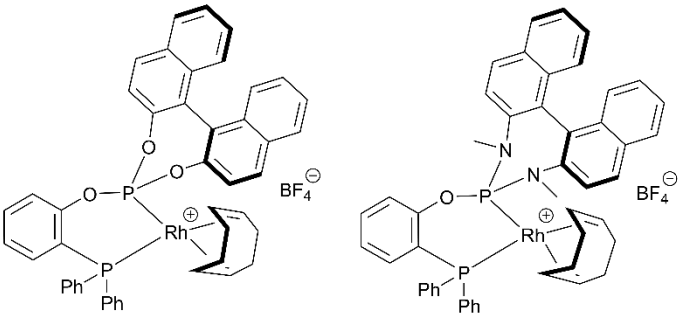

C1 **C2**

Figure 4: Rh complexes with P-OP' ligands used in this project.

The effectiveness of these complexes is based in several factors, all of which are not yet fully understood, but several studies show that the reactivity of the complexes can be more or less predicted taking into account electronic and steric effects[8, 20-23].

3.2.1.1. Electronic properties

Ligands **L1** and **L2** bear a phosphine moiety, which can be considered a good σ-donor, and a **POX** (X = O_2 (**L1**), $(NMe)_2$ (**L2**)) moiety, which —due to the highly electronegative O and N atoms— are considerably less electron rich and weaker σ-donors but better π-acceptors. Hence the fact that the *d*(Rh–**POX**) —2.164 Å— is smaller than *d*(Rh–**P**)[20] —2.278 Å—, which is an effect of backdonation. This can be appreciated in Figure 5, where the crystal structure of **C1** —obtained in a previous work[24] by Roger Estalella— is shown. This fact is of critical importance because it has been shown that the olefin of the substrate shows a clear electronic preference towards bonding in *cis*- with the **POX**[8, 20, 22, 23, 25, 26].

3.2.1.2. Steric properties

In addition to the game-changing effects of the electronic properties of the POX moiety, the phosphite moiety and the phenylene backbone of the ligands also play an important role by means of steric effects. The rigidity of the phenylene backbone constrains the flexibility of the ligand[27]

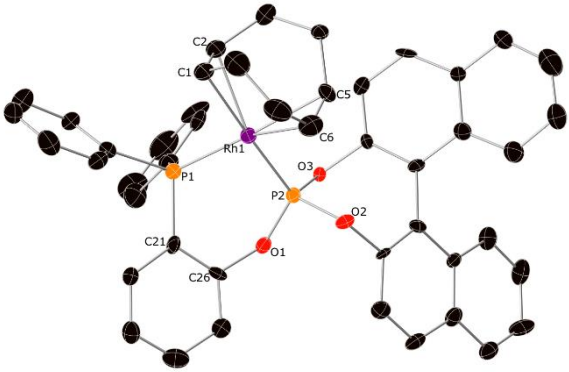

Figure 5: ORTEP representation (ellipsoids drawn at 50% probability level) of complex **C1**. The H atoms and the BF_4 anion have been omitted for clarity.

and confers the ligand a narrow bite angle (85º)[24]. The phenyl groups of the phosphine, on the other side, create a steric hindrance that can difficult the approach of the olefin from that side.

3.2.1.3. Quadrant diagram

Knowing the electronic and steric properties of the ligand, a quadrant diagram (Figure 6) can be elaborated in order to organize the information and visually assess how the substrate is going to coordinate. These quadrant diagrams were originally developed by Knowles[2] and are very useful to represent the coordination of the substrate, but it also has to be taken into consideration that they are far from perfect and cannot be taken for granted[28]. Hence, these diagrams, albeit

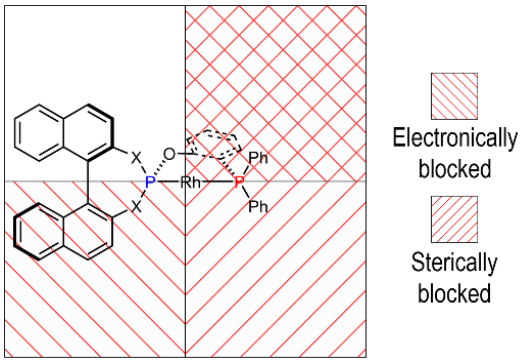

Figure 6: Quadrant diagram for complexes **C1** and **C2**.

widely used within metal-catalyzed asymmetric hydrogenation papers, have to be regarded as a way to understand how the complexes coordinate, but not as an unquestionable truth.

With this diagram, it can be seen that the upper left manifold is the more favored for olefin coordination, and thus it can be used to predict the absolute configuration of the hydrogenated substrates.

3.2.2. Methylene bridged phosphines

Methylene bridged phosphines are ligands that have a $–CH_2–$ linker between the two phosphine groups that make up the ligand. Several Rh complexes bearing this type of ligands have given excellent results in the asymmetric hydrogenation of a myriad of substrates. Some of these ligands are MiniPHOS[15, 29], TriChickenFootPHOS (TCFP)[13] and MaxPHOS[6, 30], amongst some others (Figure 7). It should be noted that MaxPHOS has a –NH– linker instead of a methylene, which makes its synthesis more versatile. The chirality of these ligands stems from the phosphorus atom, which is *P*–stereogenic unlike ligands **L1** and **L2**, in which the chiral element can be found in the 1,1'-binaphtyl group. In this work ligand **L3** will be used to synthesize the bischelate complex **C3** (Figure 8). **L3** has a *P*–stereogenic phosphine with a phenyl and a 9-phenanthryl moiety on one side of the bridge, and a phosphine with two phenyl groups on the other.

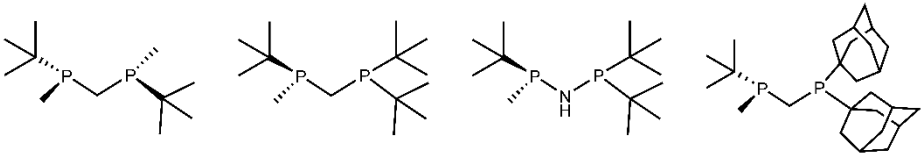

Figure 7: Some examples of diphosphines with a single-atom linker.

3.2.2.1. Structural properties

Because **L3** lacks electronegative atoms like the phosphites in **C1** and **C2**, it is electron richer than the **P–OP'** ligands. However, the main trait of this ligand is its narrow bite angle, that in similar diphosphines it has been reported to be around 70º, depending on the phosphine[6, 31]. Such small bite angles produce less steric hindrance, as the "cone" formed by the P–M–P occupies less space. This fact allows for the formation of structurally uncommon complexes, as the metal is able to coordinate two molecules of the same ligand (**C3**).

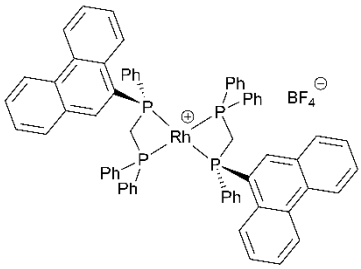

C3

Figure 8

*3.2.2.2. Coordination of **L3***

These ligands often form standard chelated complexes (Figure 9), which are quite strained. However, the narrow bite angle of the ligands also favors the formation of other structures, like binuclear complexes in which the diphosphine acts as a bridge —also known as an A-frame— between the two metals[32]. This kind of behavior, when a donor moiety of a bi- or a polydentate ligand decoordinates relatively easily, is called hemilability.

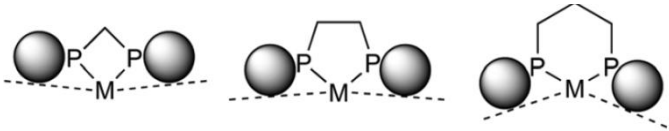

Figure 9: Steric effects of the bite angle *(image from Mansell et al., ref. 31)*.

In the case of MiniPHOS, Imamoto *et al.* reported that when using $[Rh(nbd)_2]^+$ the bischelated complex was formed[4], but when they used $[Rh(COD)_2]^+$ the monochelated complex was obtained[33] (Scheme 1), regardless of the stoichiometry. Hence, the coordination chemistry of **L3** could depend on the lability of the stabilizing ligand, being nbd easier to substitute[34] and thus facilitating the formation of the bischelate. It is worth noting that the bischelated complexes can achieve results as good or better than those obtained with monochelated complexes bearing the same ligand, although much slower conversion has been observed[4].

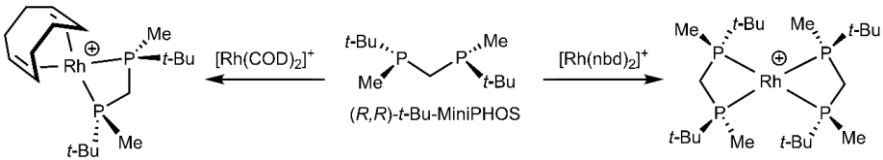

Scheme 1: Formation of a monochelated or bischelated complexes with the MiniPHOS ligand.

3.3. HYDROGENATION

3.3.1. Mechanism

In order to design highly effective ligands and to achieve optimal results in conversion and enantioselectivity the mechanism of hydrogenation must be fully understood. Unfortunately, and despite many efforts and papers dedicated to the study of the mechanism of Rh-catalyzed hydrogenation, still no completely general statements can be made. Overall, it is known that there are two possible mechanisms through which the hydrogenation of functionalized olefins is attained, and both involve an additive oxidation step, the coordination of the substrate with the Rh to form a chelated adduct, and the subsequent reductive elimination, where the hydrogenated substrate is produced. The differences lie in the order of the first two steps. The two mechanisms can be seen in Figure 10.

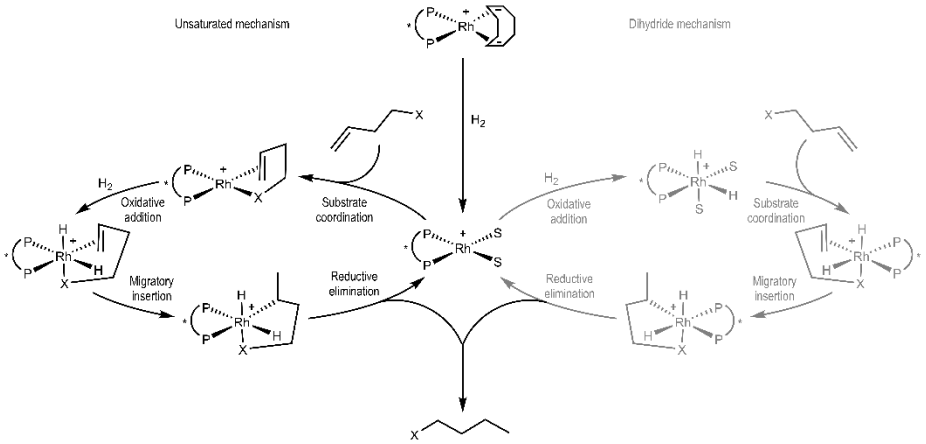

Figure 10: The two accepted mechanisms for Rh-catalyzed hydrogenation.

In the *unsaturated mechanism*, which was the first one to be proposed, the olefin coordinates in the first place substituting the ancillary ligand of the complex (usually COD or nbd, which is hydrogenated in the first term) in the square planar geometry. Then, the additive oxidation happens and Rh(I) oxidizes to Rh(III) and acquires an octahedral geometry. This is the mechanism expected to be followed by **C1** and **C2**, the ones bearing **P–OP'** ligands[8].

In the *dihydride mechanism*, the first step is the oxidative addition of H_2 on Rh, and later the olefin is coordinated to the octahedral complex. This has been demonstrated to be the mechanism followed by electron-rich, bis(trialkylphosphines),[8] including diphosphines with

C_1-linkers[4, 11, 15, 35-37]. This is not the case for ligand **L3**, that has four aryl substituents, hence making it considerably more electron-poor. Thus, an unsaturated mechanism should be expected for **C3**, in the same way as with the **P–OP'** ligands. In this case, however, the substrate coordinates to the complex after two phosphine groups (one for each chelate) dissociate form the Rh and generate two vacancies, according to a mechanistic study by Imamoto and Gridnev[36], although the intermediates with the complex–substrate adduct could not be detected.

3.3.2. Important parameters

In asymmetric hydrogenation with organometallic catalytic precursors, there are certain parameters to take into account in order to assess whether the complexes could have a potential for industrial applicability. The main parameters that have to be taken into consideration are:

- Conversion: It indicates the amount of substrate that has been hydrogenated by the catalyst after a certain time. It is usually determined by chromatography or NMR.
- Enantiomeric excess: It measures the optical purity of the chiral product. It indicates how much more of an enantiomer there is in relation with its counterpart. For the substrates of this project, it is determined *via* HPLC or GC with a chiral column.
- Substrate to catalyst ratio (S/C): It is the amount of catalyst needed to hydrogenate a certain amount of substrate. Industrially, a similar information can be obtained with the turnover number (TON), which represents the number of moles of substrate that a mole of catalyst can hydrogenate.
- Reaction time: The time that a catalyst takes to hydrogenate all of the substrate. It is of the utmost importance, as a catalyst that albeit effective takes a very long time to perform the hydrogenation cannot be used in industry. Following the same concept as with the TON, reaction time is measured industrially with the turnover frequency (TOF), which measures the number of turnovers per unit of time.
- H_2 pressure: Catalysts that are able to function under less than 5 bar of H_2 are the best regarded because they do not require expensive high-pressure facilities to be applied industrially[12].
- Solvent: Being able to perform hydrogenations using environmentally friendly solvents (i.e. non chlorinated solvents), like water or methanol, is in one of the industries' best interests[38].

- Temperature: Energy-wise, the best possible outcome is that a hydrogenation reaction is performed at room temperature. Luckily, this is the most common case in asymmetric catalysis, because asymmetric induction improves at low temperature and the catalysts do not stand harsh conditions.
- Catalyst immobilization: In the world's pursue for a greener chemistry, great effort has been put into researching new ways of carrying out metal-catalyzed asymmetric hydrogenations. One of these new methods is supporting the complexes onto resins[39], although advances significant enough as to implement these methods at an industrial scale have not been yet made. However, it is still worth mentioning, as the development of greener methods is one of the challenges of contemporary homogenous catalysis.

4. OBJECTIVES

The original objectives of the experimental TFG were:

1. Synthesis and characterization of a new chiral methylene-bridged diphosphine (**L3**).
2. Synthesis of **C3**, a cationic rhodium(I) complex derived from **L3**.
3. Asymmetric hydrogenation of substrates **S1**–**S12** with complexes **C1**–**C3**.

Due to the exceptional circumstances derived from the covid19 pandemics, only objectives 1 and 2 could be tackled and therefore objective 3 was reformulated as:

3'. A literature analysis of the results on the hydrogenation of substrates **S1**–**S12** with similar catalysts in order to conduct a comparison in the future, once catalysts **C1**–**C3** have been tested.

5. SYNTHESIS AND CHARACTERIZATION OF L3

5.1. SYNTHESIS

The synthesis of **L3**, a methylene-bridged diphosphine, was carried out following the previous work of the Homogenous Catalysis group at the department of Inorganic and Organic Chemistry[40]. The boronated derivative, **L3·BH$_3$**, was prepared by reaction between deprotonated methylphosphine–borane **P3** and chlorodiphenylphosphine (Scheme 2), followed by the protection with excess of borane. Related methods have been used previously in the synthesis of many similar and well-known ligands, like TCFP[5] or MiniPHOS[41].

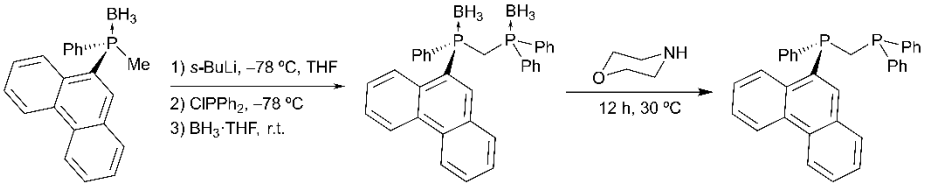

P3 **L3·BH$_3$** **L3**

Scheme 2: Synthesis of **L3**.

The deprotonation of the methylphosphine-borane **P3** was performed using *s*-BuLi at –78 ºC. This is the typical procedure in the literature for this reaction[4, 42], although another method developed by Jugé *et al.*[43] using *n*-BuLi at room temperature has also been tested in the previous work[40] of the group with similar phosphines, but was dismissed for this project because the original method rendered a better yield.

Then, the carbanionic phosphine-borane was treated with chlorodiphenylphosphine at –78 ºC and then with an excess of BH$_3$·THF to yield the protected diphosphine–borane, which was then recrystallized in dichloromethane/hexane. The final product **L3·BH$_3$** was an air-stable white solid in a 78% yield.

In order to synthesize **C3**, **L3·BH$_3$** had to be deprotected first, otherwise the borane would reduce the Rh to its metallic form[44]. This was done *via* a basic pathway with morpholine[45], although an acidic method has also been described[46]. The latter has been usually applied to

trialkylphosphines —like MiniPHOS[41]— with good results, but previous research within this group indicates that the basic method might be the most appropriate with less electronically rich diphosphines[40]. The deboronation[47] was carried out by stirring the protected phosphine with 5 mL of morpholine overnight at 30 ºC. The solution was then eluted with toluene though an alumina column and the obtained product **L3** was an air-sensitive white pasty solid.

5.2. CHARACTERIZATION

L3·BH$_3$ was characterized by ^{1}H NMR, ^{31}P{^{1}H} NMR, IR, HRMS and EA. The NMR spectra confirmed the expected structure of the diphosphine-borane and its purity. Broad peaks in the ^{31}P{^{1}H} spectrum (Figure 11) were observed and confirmed the coupling of the phosphorus to the boron. The expected intense B–H bands were visible at the IR spectra, at 2382 cm^{-1}. The EA showed similar percentages of C and H to those expected, within 2% of error range.

The ^{31}P{^{1}H} NMR spectrum showed two broad peaks at +16.7 and +15.4 ppm that corresponded to each phosphine moiety, with that at higher field one corresponding to the *P*–stereogenic phosphorus. The coupling between the two phosphorus atoms could not be observed due to the broadening of the peaks because of the quadrupolar spin of boron. The expected doublets could be clearly seen in Figure 11 for the deprotected ligand.

The ^{1}H NMR spectrum (Figure 12) shows an aromatic region at 9–7 ppm corresponding to the three phenyl groups and the 1-phenanthryl unit. At 3.8–3.4 ppm two multiplets can be observed that correspond to the two protons of the methylene bridge. These are very diagnostic peaks, as they show that the methylphosphine and the chlorodiphenylphosphine reacted correctly.

The free diphosphine **L3** was characterized by ^{1}H, ^{31}P{^{1}H} and ^{13}C{^{1}H} NMR spectroscopy. In the ^{31}P{^{1}H} spectrum (Figure 11), the doublets mentioned in Section 5.2 can be perfectly observed, confirming that both borane protecting groups have been removed. Both peaks appear now at much higher fields, at negative chemical shifts, with the *P*-stereogenic phosphorus appearing at –30.5 ppm and the other one at –22.2 ppm. The $^2J_{PP}$ was 131.4 Hz. A small roof effect could be observed.

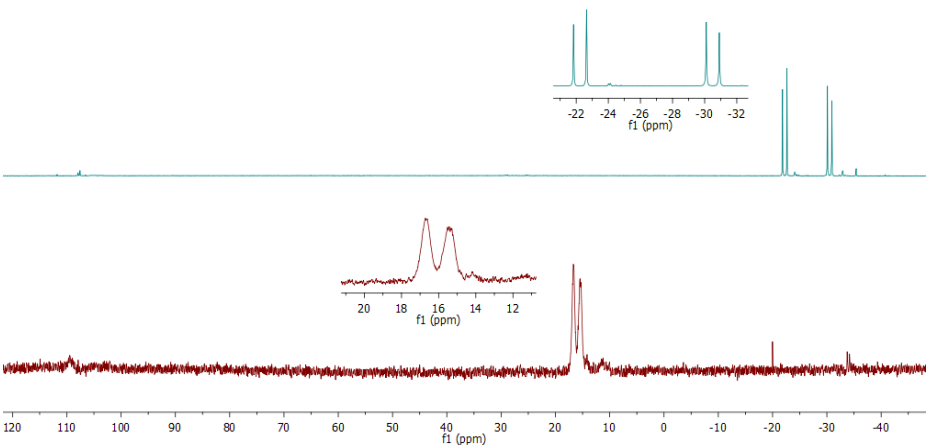

Figure 11: $^{31}P\{^{1}H\}$ spectra of **L3·BH$_3$** (bottom) and **L3** (top).

The ^{1}H NMR spectrum of the free diphosphine (Figure 12) shows a very similar disposition to that of the protected diphosphine, although the peaks are strongly displaced towards higher fields. The methylene bridge is observed at 2.85–2.65 ppm, almost one ppm at higher field than **L3·BH$_3$**. Furthermore, the peaks do not form a multiplet system like in the previous case, and instead it can be clearly seen that they form two doublets of triplets, one for each proton of the bridge, which is coupling with its geminal proton (doublet) and with the two phosphorus (triplet).

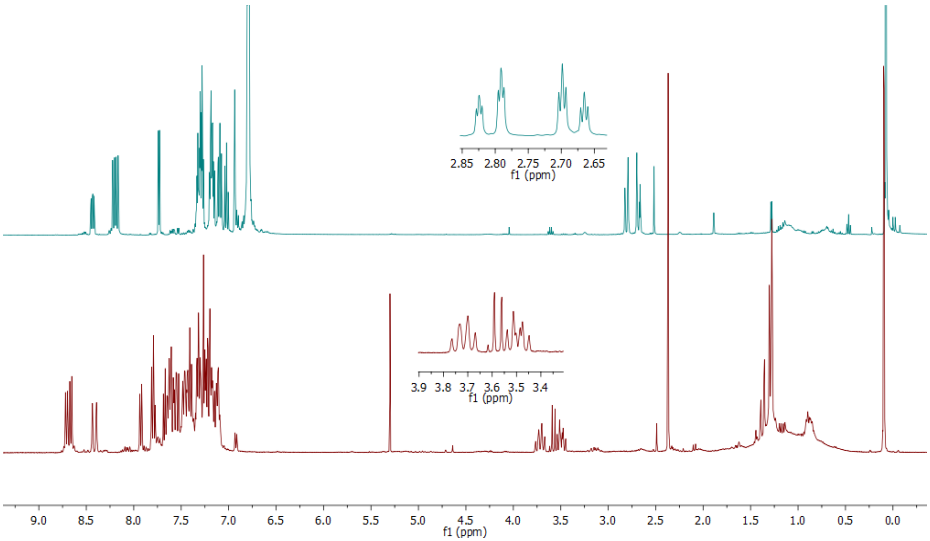

Figure 12: ^{1}H spectra of **L3·BH$_3$** (bottom) and **L3** (top).

The $^{13}C\{^1H\}$ spectrum (Figure 13) shows a triplet at 28.7 ppm (J_{CP} = 24.4 Hz) that corresponds to the coupling with the two phosphorus. The fact that it shows a triplet instead of a doublet of doublets is because the two phosphorus atoms bear fairly similar substituents: a methylene and two aryl groups.

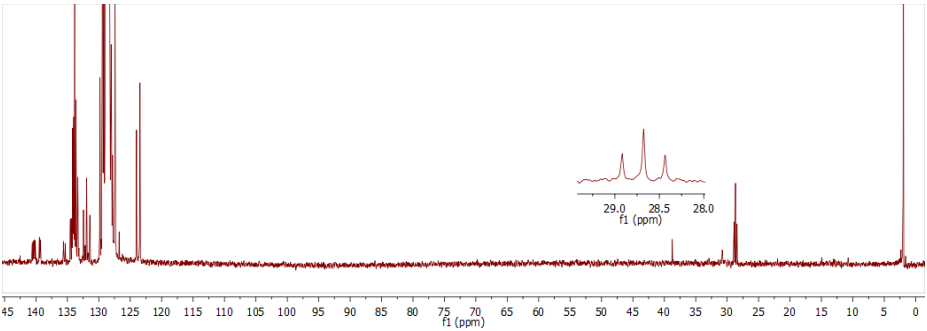

Figure 13: $^{13}C\{^1H\}$ spectrum of **L3**.

6. SYNTHESIS AND CHARACTERIZATION OF C3

With ligand **L3** in hand, the synthesis of the Rh complex **C3** was developed. The objective was the synthesis of [Rh(**L3**)(COD)]BF_4 (**C3***, Figure 14), but instead the bischelated complex [Rh(**L3**)$_2$]BF_4 was obtained (Scheme 3). However, this fact is not of much concern, as some examples can be found in the literature[4, 36, 41] where similar bischelated compounds have been tested for asymmetric hydrogenation and their results have been even better than the ones obtained with the monochelated, albeit the reaction rates were lower.

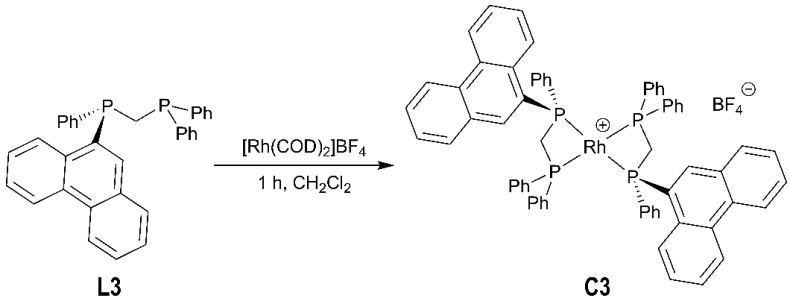

Scheme 3: Synthesis of **C3**.

6.1. SYNTHESIS

The ligand **L3** was reacted with one equivalent of $[Rh(COD)_2]BF_4$ in order to obtain the monochelated complex **C3***, still bearing a coordinated COD ligand (Figure 14). However, even at this ratio the bischelate **C3** formed, as it has also been reported in the literature[41]. To perform the complexation, the free ligand and the $[Rh(COD)_2]BF_4$ were stirred in dichloromethane during 1 h under a nitrogen atmosphere at room temperature. The obtained yellowish-orange solid was then recrystallized in dichloromethane/diethyl ether in order to recover a purer product.

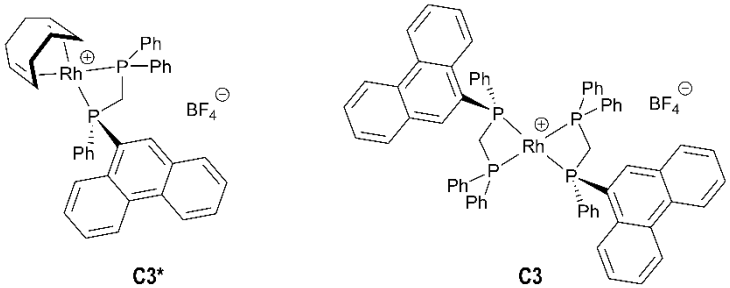

C3* **C3**

Figure 14: Expected structure (**C3***) and obtained structure (**C3**) of the complex.

6.2. CHARACTERIZATION

The complex **C3** was characterized by ^{19}F, $^{31}P\{^1H\}$ and ^1H NMR prior to recrystallization. ^1H NMR showed the presence of peaks associated to free COD[48] and $[Rh(COD)_2]BF_4$[49], already pointing to the fact that the expected monochelated complex had not been formed. After recrystallization, HRMS showed an intense peak of 1071.2071 g/mol, which corresponds to the mass of the $[Rh(\mathbf{L3})_2]^+$ fragment, and thus the suspected bischelated coordination was confirmed.

The ^1H spectrum (Figure 15) shows a group of peaks at around 2.5 ppm that most probably correspond to the methylene bridge, although they cannot be integrated reliably due to some overlapping with $[Rh(COD)_2]BF_4$ that has remained even after recrystallization.

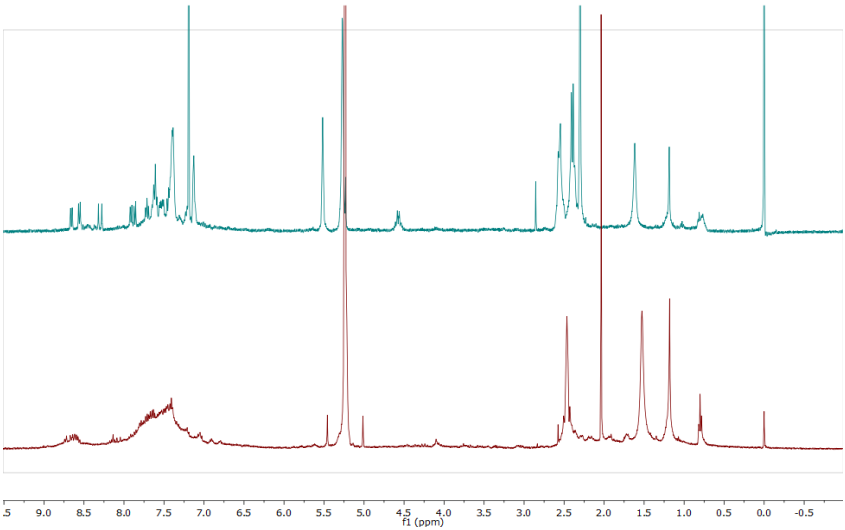

Figure 15: ^{1}H NMR spectra of **C3** before recrystallization ($CDCl_3$, top) and after (CD_2Cl_2, bottom).

The $^{31}P\{^{1}H\}$ spectrum (Figure 16) was very diluted and thus difficult to interpret. On top of that, the bischelate can show two coordination modes: *trans* (C_2-symmetric) and *cis* (C_1-symmetric) (Figure 17). The two groups of signals around –30 ppm are very likely to correspond to one or a mixture of the two bis(chelated) complexes[50].

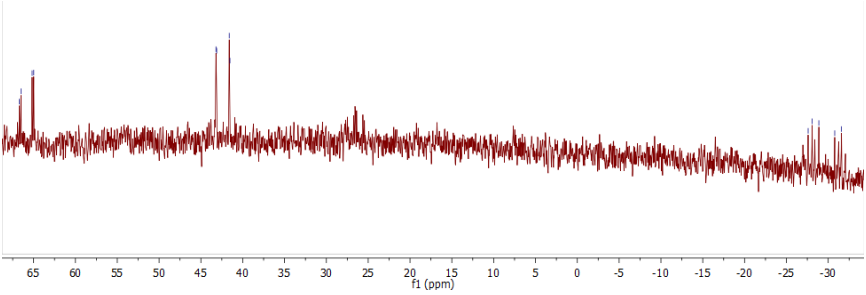

Figure 16: $^{31}P\{^{1}H\}$ spectrum of **C3**.

Furthermore, two doublets of doublets can be observed at +65.8 and +42.4 ppm, at much lower fields than those expected for diphosphine chelates[50]. These peaks, according to literature[51, 52], could correspond to chelated complexes with monooxidized diphosphines. The fact that the HRMS showed a peak for the exact mass of the bischelated complex suggests that the phosphine could be oxidized in solution. The possibility of having both the phosphorus of the

diphosphine oxidized was discarded due to the lack of peaks in the 20–30 ppm region[53, 54]. From previous experience in the group, it can be hypothesized that the oxidized phosphorus was the one with the 1-phenanthryl moiety. However, further characterization should be done to confirm this fact. This reasoning leads to two possible structures for complex **C3'** (Figure 17), in the same manner as it has been proposed for the non-oxidized bischelate **C3** earlier[55].

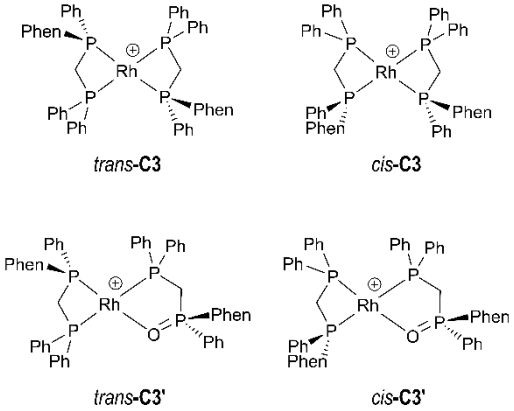

Figure 17

Due to the covid19 pandemic, no further characterization could be carried out in order to better elucidate the structure of **C3'**. An attempt at growing crystals for X-ray analysis had been made at the moment that the experimental work had to be stopped. In the future, due to its tendency to oxidize in solution, the synthesis and purification of **C3** will be done under strict exclusion of air.

7. BIBLIOGRAPHIC ANALYSIS OF THE HYDROGENATION OF SUBSTRATES S1–S12

The substrates of Figure 2 could not be hydrogenated with complexes **C1**–**C3** due to the outbreak of the covid19 virus. Instead, examples of previous hydrogenations with similar catalysts found in the literature are presented in order to build a robust database and to try to predict how the asymmetric hydrogenations could turn out with our catalysts. Of course this is at best

speculative because of the poor mechanistic knowledge despite the many efforts that have been put into its elucidation with a vast amount of substrates[14, 15, 35, 56, 57]. To this day, a general rational design strategy for ligands has not been achieved, and ultimately the only way of proving their efficacy is through experimental testing[58]. The data gathered in the next sections, however, will help to put the results of our catalysts in context once the hydrogenations are carried out.

7.1. General procedure

In this section, results from different studies will be presented in a table, one for each compound or group of compounds. The same criteria have been applied when analyzing the papers in order to obtain fairly comparable data. The criterion that has been given the highest importance is ligand similarity, meaning that the results that were obtained using ligands very similar to **L1–L3** have received the most relevance. The complete list of the ligands is given in Appendix 1. Following this criterion, in order of importance, the other criteria have been *ee* (% and *R*/*S*), conversion (%), substrate to catalyst ratio (S/C), time (h), H_2 pressure, solvent and temperature.

7.2. (Acetamido)dehydroamino acids (S1–S5)

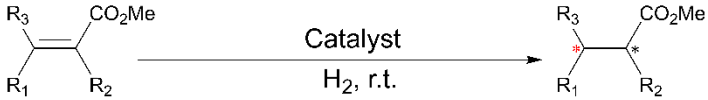

S1: R_1 = Ph, R_2 = NHAc, R_3 = H; **S2**: R_1 = H, R_2 = NHAc, R_3 = H; **S3**: R_1 = 4-FC_6H_4, R_2 = NHAc, R_3 = H; **S4**: R_1 = Ph, R_2 = CH_2NHAc, R_3 = H; **S5**: R_1 = NHAc, R_2 = H, R_3 = Me

Entry	Subst.	S/C	t (h)	Solvent	H_2 pres. (bar)	Conv. (%)	ee (%)	Ligand	Ref.
1[(a)]	**S1**	100	1	CH_2Cl_2	3.15	100	81 (*S*)	**L1**	24
2[(a)]	**S1**	100	1	CH_2Cl_2	3.15	100	85 (*R*)	**L2**	24
3[(a)]	**S2**	100	1	CH_2Cl_2	3.15	100	91 (*R*)	**L1**	24
4[(a)]	**S2**	100	1	CH_2Cl_2	3.15	100	57 (*R*)	**L2**	24
5	**S3**	100	12	THF	20	>99	99 (*R*)	**L4**	8
6	**S4**	100	18	CH_2Cl_2	10	38	87	**L5**	59
7	**S5**[(b)]	100	18	CH_2Cl_2	10	5	29 (*R*)	**L5**	59
8	**S1**	10000	43	MeOH	5	>99	99 (*S*)	**L6**[(c)]	6
9	**S2**	10000	16	MeOH	5	>99	99 (*S*)	**L6**[(c)]	6
10	**S3**[(d)]	100	1	MeOH	3	99	99.2 (*R*)	**L7**[(e)]	60

11	**S4**	–	–	–	–	–	–		–
12	**S5**	333	16	MeOH	5	>99	99 (*S*)	**L6**[(c)]	6

(a) These data correspond to the previous work of this group using **C1** and **C2**.
(b) The (Z)-isomer, much more challenging, was hydrogenated instead of the (*E*)-isomer.
(c) MaxPHOS.
(d) 3,5-$F_2C_6H_3$ instead of 4-FC_6H_4.
(e) BulkyP*.

Table 1: Asymmetric hydrogenation results of substrates **S1**–**S5**. Entries 1–7 correspond to **P–OP'** ligands while Entries 8–12 correspond to diphosphines with a C_1-linker.

As it can be seen in Table 1, α- and β-(acetamido)dehydroamino acids are very well-known substrates and in most cases give almost perfect enantioselectivities and full conversion. In some cases, like Entries 8 and 9, excellent results were accomplished even at a S/C ratio of 10000, an extremely high number. Of course, achieving full conversion with those conditions required a long reaction time, but within that same article, with a S/C of 100, the same results were obtained in 10 minutes[6]. Similar results were obtained with other C_1-linked diphosphines[4, 41], and even with commercially available ones like TCFP[5, 35].

Entries 1–4 correspond with the results obtained two years ago with catalysts **C1** and **C2**[24], belonging the results of 1 and 3 to the former and 2 and 4 to the latter. Even though better results have been obtained with **P–OP'** complexes in the asymmetric hydrogenation of **S1** and **S2**, the results of **C1** and **C2** are shown because they are the ones that would have been obtained, had the hydrogenations been repeated for this project. It is worth mentioning the work of Pizzano and Barbaro[39] where they hydrogenated substrates **S1** and **S2** with **C1**. The peculiarity of this work was that the catalysts were supported to an ionic resin, and thus the hydrogenation could be carried out in water, where it performed really well (full conversion, 89% *ee* for **S1** and 84% *ee* for **S2**), although it took a longer time.

For **S4**, no articles have been found in the literature where its hydrogenation is performed by a C_1-linked diphosphine, and just the one example has been found for the **P–OP'** ligand. Some results have been found for other phosphine ligands[61-63], but they are not commented because they are very different to ligands **L1**–**L3**.

In the case of **S5**, it can be observed that the MaxPHOS ligand (**L6**) performed much better than the **P–OP'** ligand. On one hand, it has to be mentioned that the **P–OP'** ligand was tested with the (*Z*)-**S5** isomer instead of with (*E*)-**S5**. The former is much more challenging due to steric effects, so a better performance should be expected with the latter isomer. However, it should

also be pointed out that MaxPHOS was also tested with the (*Z*)-**S5** isomer and gave the same results as with its counterpart, and thus it is arguably the best catalyst of the two compared for **S5**.

7.3. ITACONIC ACID DERIVATIVES (S6–S7)

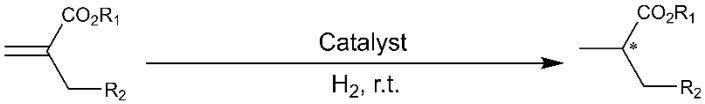

S6: R_1 = Me, R_2 = CO_2Me; **S7**: R_1 = H, R_2 = Ph

Entry	Subst.	S/C	t (h)	Solvent	H_2 pres. (bar)	Conv. (%)	*ee* (%)	Ligand	Ref.
1[(a)]	**S6**	1000	2	CH_2Cl_2	3.15	100	92 (*R*)	**L1**	24
2[(a)]	**S6**	100	3	CH_2Cl_2	3.15	100	66 (*R*)	**L2**	24
3	**S7**	100	12	THF	20	>99	15 (*S*)	**L4**[(b)]	64
4	**S6**	10000	0.3	MeOH	5 atm	100	99.3 (*S*)	**L7**[(c)]	60
5	**S7**	–	–	–	–	–	–		–

(a) These data correspond to the previous work of this group using **C1** and **C2**.
(b) **P–OP'** ligand with the same BINOL moiety as **C1**.
(c) BulkyP*.

Table 2: Asymmetric hydrogenation results of substrates **S6**–**S7**. Entries 1–3 correspond to **P–OP'** ligands while Entries 4–5 correspond to diphosphines with a C_1-linker.

The reported results for the asymmetric hydrogenation of itaconic acid derivatives are shown in Table 2. In the case of dimethyl itaconate (DMI, **S6**), which has been widely used as a benchmark substrate for asymmetric hydrogenations, many interesting bibliographical references can be found, both for **P–OP'** ligands[7, 8, 21-23, 65-67] as for single-atom linked diphosphines[6, 35, 60]. However, for the same reason as with Entries 1–4 from Table 1, the results from the performance of **C1** and **C2** have been shown instead. Nonetheless, it is worth noting some extremely good results from similar ligands, like in the work of Pizzano[68], who reported full conversion and 99.6% *ee* with a S/C of 10000 with a **P–OP'** ligand with a phenylene backbone, as in **C1**. On the other hand, as it can be seen, even better results were accomplished with BulkyP* (**L7**), a methylene-bridged diphosphine that has also achieved great results with substrates **S1**–**S3** and **S5**. On top of that, in the same paper[60] cited in Table 2 an enantioselectivity of 99.0% was obtained with a S/C of 200000, which ranks among the best results ever obtained in a Rh-catalyzed asymmetric hydrogenation[69].

In contrast to **S6**, **S7** has been very scarcely studied, with no examples in the literature of the asymmetric hydrogenation of this substrate with diphosphines with single-atom linkers. For **P–OP'** ligands, only one example has been found and, as it can be seen, it is not very good. This fact is well-justified because the presence of only a carboxylate group seldom favors the formation of a chelate in the Rh–substrate adduct. It is true that enantioselectivities up to 98.5% *ee* have been achieved[70, 71], but with Ir and Ru complexes bearing very different ligands, and thus the results are not comparable.

7.4. CYCLIC ENAMIDES (S8–S9)

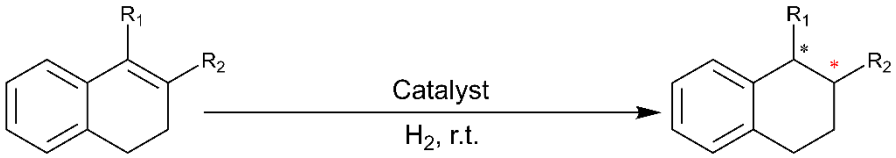

S8: R_1 = NHAc, R_2 = H; **S9**: R_1 = H, R_2 = NHAc

Entry	Subst.	S/C	t (h)	Solvent	H_2 pres. (bar)	Conv. (%)	*ee* (%)	Ligand	Ref.
1	**S8**	100	18	THF	20	>99	88 (*R*)	**L8**[(a)]	7
2	**S9**	100	21	CH2Cl2	20	18	68 (*S*)	**L9**[(b)]	14
3	**S8**	100	0.8–1.5	MeOH	2	>99	75 (*S*)	**L6**[(c)]	6
4	**S9**	333	>9	MeOH	10	>99	99 (*S*)	**L6**[(c)]	72

(a) **P–OP'** ligand with the same BINOL moiety as **C1**.
(b) **P–OP'** ligand with the same phenylene backbone as **C1** and **C2**.
(c) MaxPHOS.

Table 3: Asymmetric hydrogenation results of substrates **S8**–**S9**. Entries 1–2 correspond to **P–OP'** ligands while Entries 3–4 correspond to diphosphines with a C_1-linker.

In Table 3 the asymmetric hydrogenation results of cyclic enamides **S8** and **S9** are presented. These family of compounds are well-known for being difficult substrates[61]. Despite this fact, extensive research has permitted the obtention of improved results over time. In the case **S8**, MaxPHOS (**L6**) does not yield remarkably good results, although it can be considered that good enantioselectivity is achieved. The **P–OP'** ligand in Entry 1 —a ligand with the same BINOL moiety as **C1** but with an oxymethylene bridge— yields slightly better results, which is surprising because up until this case all diphosphines with single-atom linkers had outperformed the phosphine–phosphite ligands with similarities to **C1**–**C2**. However, other similar phosphine–phosphites have failed to provide such good results[8]. It is interesting to note that the results

obtained when trying to obtain the (*S*)-enantiomer with the same ligand but with an (R_a)-BINOL moiety in the phosphite, the performance was much poorer. This was because of the well-known matched-mismatched effect in catalysis[73] when the ligand contains more than one stereogenic element.

In the case of **S9**, the results with the **P–OP'** ligand are not so good. It should be remarked that **S9** has been considerably less studied than **S8**, and that the result shown in the Entry 2 is the only one reported for the asymmetric hydrogenation of this substrate with a **P–OP'** ligand. On a completely opposite side, the enantioselectivity results obtained with MaxPHOS (**L6**) for **S9** are the best ones yet[72].

From the little amount of data available with this type of substrate, it is clear that more research is needed in order to attain better results. For this reason, it is important to expand the range of ligands tested with this type of substrate, and the results with precursors **C1**–**C3** could be of interest.

7.5. KETIMINES (S10–S11)

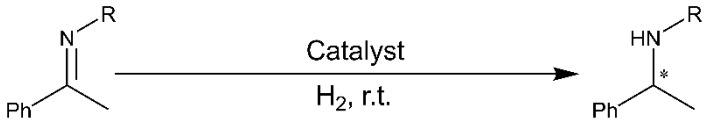

S10: R = Ph; **S11**: R = 4-ClC$_6$H$_4$

Entry	Subst.	S/C	t (h)	Solvent	H_2 pres. (bar)	Conv. (%)	*ee* (%)	Ligand	Ref.
1	**S10**	100	20	MeOH	50	>99	39 (*R*)	**L4**[(a)]	74
2	**S10**	100	24	CH2Cl2	30	100	36 (*R*)	**L9**[(b)]	75
3	**S11**	100	16	MeOH	50	21	9 (*S*)	**L10**[(c)]	17
4	**S10**	200	1.5	CH2Cl2	1 atm	91	86[(d)]	**L11**[(e)]	76
5	**S11**	200	12	CH2Cl2	1 atm	99	83[(d)]	**L11**[(e)]	76

(a) **P–OP'** ligand with a BINOL moiety like **C1**.
(b) **P–OP'** ligand with a phenylene bridge like **C1** and **C2**.
(c) Phosphine–phosphinite ligand.
(d) The enantiomeric conformation was not determined.
(e) BisP* ligand, similar to MiniPHOS but with an ethylene bridge.

Table 4: Asymmetric hydrogenation results of ketimines **S10**–**S11**. All hydrogenations were performed using Ir catalysts.

As it can be seen, not much information can be applied to complexes **C1**–**C3** from the results presented in Table 4 for the asymmetric hydrogenation of ketimines. This type of substrate has been traditionally hydrogenated with iridium catalysts, which due to a different mechanism[77, 78] have traditionally been used to hydrogenate unfunctionalized olefins or simple imines[12]. The table does show, however, how difficult it is to asymmetrically hydrogenate ketimines, being its most obvious example Entry 3, which achieved a very low conversion and enantioselectivity. Nonetheless, it has to be pointed out that good results have indeed been obtained with substrates **S10** and **S11**, although with very different ligands[79, 80] than those studied in this project.

With this information, it is fairly assumable that these hydrogenations should not work with the rhodium complexes studied in this project, but we think it is still worth trying in order to be able to fully discard them.

Furthermore, hydrogenation of acyclic imines is still quite understudied, and no examples can be found in the literature of their hydrogenation with diphosphines with a single-atom linker. In Table 4, Entries 4 and 5 show the hydrogenation results for *t*-Bu-BisP*, a ligand with the same substituents as *t*-Bu-MiniPHOS but with an 1,2-ethane bridge. Given the narrower bite angle of MiniPHOS and thus its more rigid structure, it would not be surprising if this ligand gave similar or even better results[31]. Thus, a future project with ligand **L3** forming an Ir complex could be very interesting, as it would firstly exemplify how C_1-linkers perform in the asymmetric hydrogenation of ketimines.

7.6. LEVETIRACETAM PRECURSOR

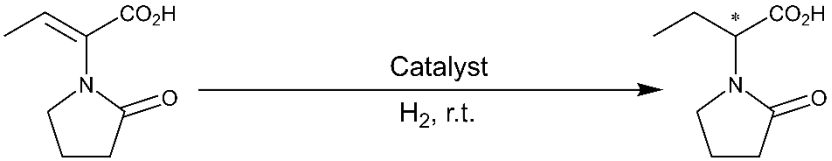

S12

Entry	S/C	t (h)	Solvent	H_2 pres. (bar)	Conversion (%)	ee (%)	Ligand	Ref.
1[(a)]	200	16	CH_2Cl_2	4 atm	100	97 (*S*)	**L12**[(b)]	81
2	100	18	THF	20	>99	99 (*R*/*S*)	**L4/L13**[(c)]	17

(a) The precursor was the amide version of **S12**.
(b) (*S*,*S*)-Et-DUPHOS.
(c) **P–OP'** ligands with a BINOL moiety such as **C1**. (R_a)-BINOL gave the *S* enantiomer while (S_a)-BINOL gave the *R* enantiomer.

Table 5: Asymmetric hydrogenation results for **S12**.

As it can be seen, the results showed in Table 5 are very good, and many other hydrogenations have been made with a plethora of ligands that rendered excellent results as well[82]. These results are not that surprising, as **S12** is, in fact, an α-(acylamino)acrylate like **S1**–**S3**, which is a very well-studied family of compounds, as it has been seen in Section 7.2. **S12** only has its own category because its classified as a direct precursor of a commercially available drug, and its purpose in this project was to exemplify the importance and potential industrial applicability of catalysts like **C1**–**C3**.

Seeing how **S12** is not generally regarded as a difficult substrate, hydrogenation results with our complexes should render fairly good results. As with the case of many other of the substrates studied, their hydrogenation with a diphosphine with a single-atom linker would have an added value due to the scarcity —or even non-existence— of examples in the literature.

7.7. OBSERVATIONS AND PREDICTIONS

From the many articles analyzed in the quest for the best asymmetric hydrogenation results of substrates **S1**–**S12** with catalysts similar to **C1**–**C3**, some conclusions can be drawn.

In most cases, ligands with single-atom bridges (similar to **L3**) have provided better results than **P–OP'** ligands with similar moieties or backbones as **C1** and **C2**. This is the case for **S3**, **S5**, **S9** and, as it has been commented, probably for **S10** and **S11**. The only exception is **S8**. For **S1**, **S2** and **S6** —being those the benchmark substrates MAC, MAA and DMI, respectively—, both types of ligands obtain the same excellent results, as these substrates have been thoroughly studied and are not considered challenging substrates. No data has been reported about asymmetric hydrogenations with diphosphines with single-atom linkers for substrates **S4**, **S7** and **S10**–**S12**, which points out to the next idea.

Diphosphines with single-atom linkers like **L3** are heavily understudied, both in comparison with **P–OP'** ligands and with diphosphines in general. This fact has no justification other than the trends that the research for diphosphorus ligands has taken over the years[83].

It has to be noted that a bibliographic research like this one has no control over each of the parameters at which the reactions were carried, and thus comparisons should be made with extreme care, as differences apparently attributable to the ligands employed could be actually caused by another factor. This is only mentioned in order to warn about how unproductive it would

be to try to make specific predictions, and to emphasize that the point of this bibliographic research is to facilitate future work on asymmetric hydrogenations with complexes **C1**–**C3**, and that by no means pretends to be a replacement of experimental work.

8. EXPERIMENTAL SECTION

8.1. MATERIALS AND METHODS

The syntheses of **L3·BH$_3$**, **L3** and **C3** were performed under a purified nitrogen atmosphere by standard Schlenk and vacuum-line techniques. The solvents were obtained from a solvent-purification system. ^{1}H, ^{13}C{^{1}H}, ^{19}F and ^{31}P{^{1}H} NMR spectra were recorded with 400 MHz spectrometers with the specified solvent. The fields are 400 MHz (^{1}H), 101 MHz (^{13}C{^{1}H}), 376 MHz (^{19}F) and 162 MHz (^{31}P{^{1}H}). High-resolution mass spectrometry analyses were performed with electrospray ionization. The chromatographic analyses of the catalytic runs were performed on GC and HPLC with the specified columns. Phosphine-borane **P3** had been prepared as previously described[47].

The data for the comparative study of Section 7 was obtained from research articles. They were obtained, in turn, from the databases Scifinder and Reaxys.

8.2. PREPARATION OF L3·BH$_3$

Phosphine-borane **P3** (157 mg, 0.5 mmol) was dissolved in 10 mL of THF and the solution was cooled to –78 ºC. *s*-butyl lithium (0.5 mL of a 1.3 M solution, 0.65 mmol) was added and the solution was left stirring for 2 h at –78 ºC. Chlorodiphenylphosphine (110 µL, 0.6 mmol) was added and the mixture was allowed to slowly reach room temperature overnight. Borane–THF solution (2 mL of a 1 M solution, 2 mmol) was added and after 30 min. 20 mL of water were carefully added. The organic solvents were removed under vacuum and the suspension was extracted with dichloromethane (3x10 mL), the combined organic fractions were washed with 100 mL of water, dried with anhydrous sodium sulfate and filtered. The solution was concentrated to dryness giving a resin, which was recrystallized in dichloromethane/hexane, yielding the desired compound as a white solid after filtration and washing with pentane. Yield: 200 mg (78%).

^{1}H NMR: 8.71 (d, *J* = 8.4, 1H$_{Ar}$), 8.66 (d, *J* = 8.4, 1H$_{Ar}$), 8.41 (d, *J* = 17.6, 1H$_{Ar}$), 7.93 (d, *J* = 7.6, 1H$_{Ar}$), 7.81-7.09 (m, 20H$_{Ar}$), 3.76-3.67 (m, 1H$_{bridge}$), 3.54-3.45 (m, 1H$_{bridge}$). **^{31}P{^{1}H} NMR:** +16.7 (s, br), +15.4 (s, br). **IR:** 3056, 2926, 2382, 1435, 1104, 1059, 957, 790, 742, 690. **HRMS:**

calcd. for $[M+NH_4]^+$ 530.2503, found 530.2515; for $[M–BH_3]^+$ 499.1910, found 499.1915. **EA:** calcd. for $C_{33}H_{32}B_2P_2$, C 77.39%, H 6.30%; found C 75.99%, H 6.79%.

8.3. PREPARATION OF L3

Ligand **L3** (102 mg, 0.2 mmol) was dissolved in 5 mL of morpholine and the solution was stirred for 14 h at 30 ºC. After this time, the excess of morpholine was evaporated *in vacuo* and the residue was filtered through an alumina pad with purified toluene in order to retain the morpholine-borane adduct. After bringing the solution to dryness, the free diphosphine was obtained as a white gummy solid. Yield was not calculated but was assumed to be 90%.

^{1}H NMR (C_6D_6): 8.43 (ddd, *J* = 8.4, 5.2, 1.2, $1H_{Ar}$), 8.21 (d, *J* = 8.4, $1H_{Ar}$), 8.18 (d, *J* = 8.0, $1H_{Ar}$), 7.73 (d, *J* = 5.6, $1H_{Ar}$), 7.34-7.26 (m, $5H_{Ar}$), 7.20-7.15 (m, $3H_{Ar}$), 7.17-7.07 (m, $2H_{Ar}$), 7.04-7.00 (m, $1H_{Ar}$), 2.81 (dt, *J* = 13.2, 2.0, $1H_{bridge}$), 2.68 (dt, *J* = 13.2, 2.0, $1H_{bridge}$). **^{13}C{^{1}H} NMR (C_6D_6):** 140.6-123.5 (m, C_{Ar}, CH_{Ar}), 28.7 (t, J_{CP} = 24.4, $CH_{2\ bridge}$). **^{31}P{^{1}H} NMR (C_6D_6):** –22.2 (d, J_{PP} = 131.4, P^2), –30.5 (d, J_{PP} = 131.4, P^1).

8.4. PREPARATION OF C3

The diphosphine was dissolved in 10 mL of dichloromethane and $[Rh(cod)_2]BF_4$ (78.2 mg, 0.19 mmol) was added. The solution was stirred for 1 h and evacuated to dryness under reduced pressure. The obtained product (70.5 mg) was dissolved in DCM/hexane and left in the fridge overnight to recrystallize. The solution was filtered through a nº 3 sintered glass funnel and washed thoroughly with pentane. Yield: 41 mg (35%).

^{1}H NMR (CD_2Cl_2): 8.64 (m, $4H_{Ar}$), 8.14 (m, $4H_{Ar}$), 7.96–6.70 (m, $40H_{Ar}$), 2.61–2.28 (m, $4H_{bridge}$). **^{31}P{^{1}H} NMR (CD_2Cl_2):** 65.84 (dd, P-***P***═*O*, $^2J_{PRh}$ = 247.1, $^2J_{PP}$ = 31.6), 42.36 (dd, ***P***–*P*═*O*, $^1J_{PRh}$ = 256.8, $^2J_{PP}$ = 13.8), –28.24 (dd, *PPh*$_2$, $^1J_{PRh}$ = 77.0, $^2J_{PP}$ = 130.4), –31.42 (dd, *PPhPhen*, $^1J_{PRh}$ = 77.8, $^2J_{PP}$ = 131.2). **^{19}F NMR:** –152.38 (s, 4F). **HRMS:** calcd. for $Rh(C_{33}H_{26}P_2)_2$ 1071.2070, found 1071.2071; for $RhC_{33}H_{26}P_2O$ 603.0514, found 603.0513.

9. CONCLUSIONS

Methylene-bridged diphosphine-borane **L3·BH_3** and the free diphosphine **L3** have been successfully synthesized and characterized. Regarding the coordination to Rh(I), the characterization data suggest the formation of the bischelated complex **C3**, although complete characterization, including the determination of its crystal structure, has not been possible due to the outbreak of covid19. However, it has been determined that a bischelate with one of the *P*–stereogenic phosphorus oxidized has been formed, indicating the air instability of the complex. Clearly, the coordination of **L3** to Rh(I) is interesting and deserves further studies.

A literature search of hydrogenation results of substrates **S1**–**S12** with similar ligands to **L1**–**L3** has been made. The data analyzed tips the balance towards thinking that diphosphines with single-atom linkers like **L3** might provide with a better performance in hydrogenating these substrates than **P–OP'** ligands like **L1** and **L2**. However, the most important conclusion that can be made from this literature search is that no rotund statement can be made without having experimentally tested the catalysts.

Future hydrogenations with the aforementioned ligands will have to be made in order to confirm or dismiss the predictions suggested for their performance.

10. REFERENCES AND NOTES

1. Smith, S. W., *Toxicol. Sci.*, **2009,** *110*, 4-30.
2. Knowles, W. S., *Acc. Chem. Res.*, **1983,** *16*, 106-112.
3. A functionalized olefin is an olefin that bears a group, often containing a carbonyl, capable of coordination to the metal so the substrate is coordinated in a bidentate fashion during the hydrogenation (see Section 3.3.1).
4. Gridnev, I. D.; Yamamoi, Y.; Higashi, N.; Tsuruta, H.; Yasutake, M.; Imamoto, T., *Adv. Synth. Catal.*, **2001,** *343*, 118-136.
5. Hoge, G.; Wu, H.; Kissel, W. S.; Pflum, D. A.; Greene, D. J.; Bao, J., *J. Am. Chem. Soc.*, **2004,** *126*, 5966-5967.
6. Cristóbal-Lecina, E.; Etayo, P.; Doran, S.; Revés, M.; Martín-Gago, P.; Grabulosa, A.; Constantino, A. R.; Vidal-Ferran, A.; Riera , A.; Verdaguer , X., *Adv. Synth. Catal.*, **2014,** *356*, 795-804.
7. Fernández-Pérez, H.; Benet-Buchholz, J.; Vidal-Ferran, A., *Org. Lett.*, **2013,** *15*, 3634-3637.
8. Fernández-Pérez, H.; Donald, S. M. A.; Munslow, I. J.; Benet-Buchholz, J.; Maseras, F.; Vidal-Ferran, A., *Chem. Eur. J.*, **2010,** *16*, 6495-6508.
9. Bravo, M. J.; Ceder, R. M.; Muller, G.; Rocamora, M., *Organometallics*, **2013,** *32*, 2632-2642.
10. Adamczyk, M.; Akireddy, S. R.; Reddy, R. E., *Org. Lett.*, **2001,** *3*, 3157-3159.
11. Gridnev, I. D.; Liu, Y.; Imamoto, T., *ACS Catal.*, **2014,** *4*, 203-219.
12. Etayo, P.; Vidal-Ferran, A., *Chem. Soc. Rev.*, **2013,** *42*, 728-754.
13. Wu, H.; Hoge, G., *Org. Lett.*, **2004,** *6*, 3645-3647.
14. Arribas, I.; Rubio, M.; Kleman, P.; Pizzano, A., *J. Org. Chem.*, **2013,** *78*, 3997-4005.
15. Gridnev, I. D.; Yasutake, M.; Higashi, N.; Imamoto, T., *J. Am. Chem. Soc.*, **2001,** *123*, 5268-5276.
16. Imamoto, T.; Tamura, K.; Zhang, Z.; Horiuchi, Y.; Sugiya, M.; Yoshida, K.; Yanagisawa, A.; Gridnev, I. D., *J. Am. Chem. Soc.*, **2012,** *134*, 1754-1769.
17. Núñez-Rico, J. L. Highly modular P-OP ligands for rhodium- and iridium-mediated asymmetric hydrogenations. URiV, 2013.
18. Fleury-Brégeot, N.; de la Fuente, V.; Castillón, S.; Claver, C., *ChemCatChem*, **2010,** *2*, 1346-1371.
19. Johannes G. de Vries, C. J. E., *The Handbook of Homogeneous Hydrogenation*. Wiley: 2006.
20. Suárez, A.; Méndez Rojas, M. A.; Pizzano, A., *Organometallics*, **2002,** *21*, 4611-4621.
21. Arribas, I.; Vargas, S.; Rubio, M.; Suárez, A.; Domene, C.; Álvarez, E.; Pizzano, A., *Organometallics*, **2010,** *29*, 5791-5804.
22. Etayo, P.; Núñez-Rico, J. L.; Vidal-Ferran, A., *Organometallics*, **2011,** *30*, 6718-6725.

23. Núñez-Rico, J. L.; Etayo, P.; Fernández-Pérez, H.; Vidal-Ferran, A., *Adv. Synth. Catal.*, **2012,** *354*, 3025-3035.
24. Estalella, R. *Synthesis, characterisation and application to asymmetric olefin hydrogenation of Rh complexes with unsymmetrical diphosphorus ligands*. TFG, UB, 2017.
25. Llorente, N.; Fernández-Pérez, H.; Núñez-Rico José, L.; Carreras, L.; Martínez-Carrión, A.; Iniesta, E.; Romero-Navarro, A.; Martínez-Bascuñana, A.; Vidal-Ferran, A., *Pure Appl. Chem.*, **2019,** *91*, 3-15.
26. Fernández-Pérez, H.; Balakrishna, B.; Vidal-Ferran, A., *Eur. J. Org. Chem.*, **2018,** 1525-1532.
27. Harvey, S.; Junk, P. C.; Raston, C. L.; Salem, G., *J. Org. Chem.*, **1988,** *53*, 3134-3140.
28. Gridnev, I. D.; Higashi, N.; Asakura, K.; Imamoto, T., *J. Am. Chem. Soc.*, **2000,** *122*, 7183-7194.
29. Gridnev, I. D.; Yasutake, M.; Imamoto, T.; Beletskaya, I. P., *Proc. Natl. Acad. Sci.*, **2004,** *101*, 5385-5390.
30. Salomó, E.; Riera, A.; Verdaguer , X., *Rev. Soc. Cat. Quím.*, **2016,** *15*, 64-71.
31. Mansell, S. M., *Dalton Trans.*, **2017,** *46*, 15157-15174.
32. Marinetti, A.; Le Menn, C.; Ricard, L., *Organometallics*, **1995,** *14*, 4983-4985.
33. Imamoto, T.; Horiuchi, Y.; Hamanishi, E.; Takeshita, S.; Tamura, K.; Sugiya, M.; Yoshida, K., *Tetrahedron*, **2015,** *71*, 6471-6480.
34. Abel, E. W., *Comprehensive Organometallic Chemistry II*. Pergamon: 2002; p 557.
35. Gridnev, I. D.; Imamoto, T.; Hoge, G.; Kouchi, M.; Takahashi, H., *J. Am. Chem. Soc.*, **2008,** *130*, 2560-2572.
36. Gridnev, I. D.; Imamoto, T., *Organometallics*, **2001,** *20*, 545-549.
37. Imamoto, T., *Chem. Rec.*, **2016,** *16*, 2659-2673.
38. Dach, R.; Song, J. J.; Roschangar, F.; Samstag, W.; Senanayake, C. H., *Org. Process Res. Dev.*, **2012,** *16*, 1697-1706.
39. Kleman, P.; Barbaro, P.; Pizzano, A., *Green Chem.*, **2015,** *17*, 3826-3836.
40. Carrasco, J.; Vidal-Ferran, A.; Font-Bardia, M.; Grabulosa, A. Palladium complexes of methylene-bridged *P*-stereogenic, unsymmetrical diphosphines, *submitted*.
41. Yamanoi, Y.; Imamoto, T., *J. Org. Chem.*, **1999,** *64*, 2988-2989.
42. Rodríguez, L.; Rossell, O.; Seco, M.; Grabulosa, A.; Muller, G.; Rocamora, M., *Organometallics*, **2006,** *25*, 1368-1376.
43. Salomon, C.; Dal Molin, S.; Fortin, D.; Mugnier, Y.; Boere, R. T.; Jugé, S.; Harvey, P. D., *Dalton Trans.*, **2010,** *39*, 10068-10075.
44. Carrasco, J. *Coordination and catalysis with non-symmetric P-stereogenic methylene-bridged diphosphines*. TFM, UB, 2019.
45. Stoop, R. M.; Mezzetti, A.; Spindler, F., *Organometallics*, **1998,** *17*, 668-675.
46. McKinstry, L.; Livinghouse, T., *Tetrahedron Lett.*, **1994,** *35*, 9319-9322.
47. Grabulosa, A.; Muller, G.; Ordinas, J. I.; Mezzetti, A.; Maestro, M. A.; Font-Bardia, M.; Solans, X., *Organometallics*, **2005,** *24*, 4961-4973.
48. Cinellu, M. A.; Minghetti, G.; Cocco, F.; Stoccoro, S.; Zucca, A.; Manassero, M.; Arca, M., *Dalton Transactions*, **2006**, 5703-5716.
49. Ensign, S. C.; Vanable, E. P.; Kortman, G. D.; Weir, L. J.; Hull, K. L., *J. Am. Chem. Soc.*, **2015,** *137*, 13748-51.

50. Garrou, P. E., *Chem. Rev.*, **1981,** *81*, 229-266.
51. Gonsalvi, L.; Adams, H.; Sunley, G. J.; Ditzel, E.; Haynes, A., *J. Am. Chem. Soc.*, **2002,** *124*, 13597-13612.
52. Blagborough, T. C.; Davis, R.; Ivison, P., *J. Organomet. Chem.*, **1994,** *467*, 85-94.
53. Gianetti, T. L.; Rodríguez-Lugo, R. E.; Harmer, J. R.; Trincado, M.; Vogt, M.; Santiso-Quinones, G.; Grützmacher, H., *Angew. Chem. Int. Ed.*, **2016,** *55*, 15323-15328.
54. Morgalyuk, V. P.; Strelkova, T. y. V.; Nifant'ev, E. E.; Brel, V. K., *Mendeleev Commun.*, **2016,** *26*, 397-398.
55. Browning, J.; Bushnell, G. W.; Dixon, K. R.; Hilts, R. W., *J. Organomet. Chem.*, **1993,** *452*, 205-218.
56. Chávez, M. Á.; Vargas, S.; Suárez, A.; Álvarez, E.; Pizzano, A., *Adv. Synth. Catal.*, **2011,** *353*, 2775-2794.
57. Rubio, M.; Vargas, S.; Suárez, A.; Álvarez, E.; Pizzano, A., *Chem. Eur. J.*, **2007,** *13*, 1821-1833.
58. Gillespie, J. A.; Dodds, D. L.; Kamer, P. C. J., *Dalton Trans.*, **2010,** *39*, 2751-2764.
59. Wassenaar, J.; Reek, J. N. H., *J. Org. Chem.*, **2009,** *74*, 8403-8406.
60. Sawatsugawa, Y.; Tamura, K.; Sano, N.; Imamoto, T., *Org. Lett.*, **2019,** *21*, 8874-8878.
61. Meeuwissen, J.; Kuil, M.; van der Burg, A. M.; Sandee, A. J.; Reek, J. N. H., *Chem. Eur. J.*, **2009,** *15*, 10272-10279.
62. Hoen, R.; Tiemersma-Wegman, T.; Procuranti, B.; Lefort, L.; de Vries, J. G.; Minnaard, A. J.; Feringa, B. L., *Org. Biomol. Chem.*, **2007,** *5*, 267-275.
63. Pignataro, L.; Boghi, M.; Civera, M.; Carboni, S.; Piarulli, U.; Gennari, C., *Chem. Eur. J.*, **2012,** *18*, 1383-1400.
64. Fernández-Pérez, H. Towards Highly Efficient Ligands For Asymmetric Hydrogenations: A Covalent Modular Approach And Investigations Into Bio-Inspired Supramolecular Strategies. ICIC-URiV, 2009.
65. Lao, J. R.; Benet-Buchholz, J.; Vidal-Ferran, A., *Organometallics*, **2014,** *33*, 2960-2963.
66. Fernández-Pérez, H.; Benet-Buchholz, J.; Vidal-Ferran, A., *Chem. Eur. J.*, **2014,** *20*, 15375-15384.
67. Kleman, P.; Vaquero, M.; Arribas, I.; Suárez, A.; Álvarez, E.; Pizzano, A., *Tetrahedron: Asymmetry*, **2014,** *25*, 744-749.
68. Suárez, A.; Pizzano, A., *Tetrahedron: Asymmetry*, **2001,** *12*, 2501-2504.
69. Li, W.; Rodriguez, S.; Duran, A.; Sun, X.; Tang, W.; Premasiri, A.; Wang, J.; Sidhu, K.; Patel, N. D.; Savoie, J.; Qu, B.; Lee, H.; Haddad, N.; Lorenz, J. C.; Nummy, L.; Hossain, A.; Yee, N.; Lu, B.; Senanayake, C. H., *Org. Process Res. Dev.*, **2013,** *17*, 1061-1065.
70. Li, J.; Shen, J.; Xia, C.; Wang, Y.; Liu, D.; Zhang, W., *Org. Lett.*, **2016,** *18*, 2122-2125.
71. Zhu, S.-F.; Yu, Y.-B.; Li, S.; Wang, L.-X.; Zhou, Q.-L., *Angew. Chem. Int. Ed.*, **2012,** *51*, 8872-8875.
72. Revés, M.; Ferrer, C.; León, T.; Doran, S.; Etayo, P.; Vidal-Ferran, A.; Riera, A.; Verdaguer, X., *Angew. Chem. Int. Ed.*, **2010,** *49*, 9452-9455.
73. The matched-mismatched effect occurs when the ligand has two or more chiral centers. In this case the chiral centers can cooperate giving better results (matched); or compete giving worse results (mismatched).

74. Núñez-Rico, J. L.; Fernández-Pérez, H.; Benet-Buchholz, J.; Vidal-Ferran, A., *Organometallics*, **2010,** *29*, 6627-6631.
75. Vargas, S.; Rubio, M.; Suárez, A.; Pizzano, A., *Tetrahedron Lett.*, **2005,** *46*, 2049-2052.
76. Imamoto, T.; Iwadate, N.; Yoshida, K., *Org. Lett.*, **2006,** *8*, 2289-2292.
77. Brandt, P.; Hedberg, C.; Andersson, P. G., *Chem. Eur. J.*, **2003,** *9*, 339-347.
78. Cadu, A.; Andersson, P. G., *Dalton Trans.*, **2013,** *42*, 14345-14356.
79. Baeza, A.; Pfaltz, A., *Chem. Eur. J.*, **2010,** *16*, 4003-4009.
80. Zhu, S.-F.; Xie, J.-B.; Zhang, Y.-Z.; Li, S.; Zhou, Q.-L., *J. Am. Chem. Soc.*, **2006,** *128*, 12886-12891.
81. Surtees, J. M., V.; Differding, E.; Zimmermann, V. 2-Oxo-1-Pyrrolydine Derivatives, Process for Preparing Them and Their Uses. WO 01/64637, 2001.
82. Friedfeld, M. R.; Zhong, H.; Ruck, R. T.; Shevlin, M.; Chirik, P. J., *Science*, **2018,** *360*, 888-893.
83. Zhou, Q.-L.; Ed., *Privileged Chiral Ligands and Catalysts*. Wiley-VCH: Weinheim, 2011.

11. ACRONYMS

COD: 1,5-Cyclooctadiene

DMI: Dimethyl itaconate

EA: Elemental Analysis

FID: Flame Ionization Detector

GC: Gas Chromatography

HRMS: High Resolution Mass Spectroscopy

HSQC: Heteronuclear single quantum coherence spectroscopy

IR: Infrared spectroscopy

MAA: methyl α-acetamidoacrylate

MAC: methyl (*Z*)-α-acetamidocinnamate

nbd: Norbornadiene

NMR: Nuclear Magnetic Resonance

TCFP: TriChickenFootPHOS

APPENDICES

APPENDIX 1: LIGANDS FROM SECTION 7

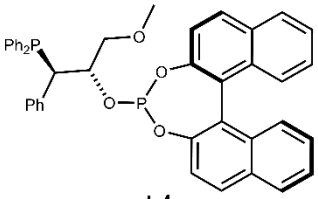

L4

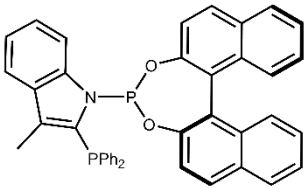

L5

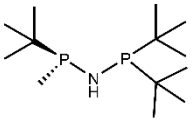

L6
(*S*)-MaxPHOS

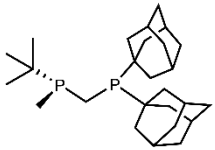

L7
(*R*)-BulkyP*

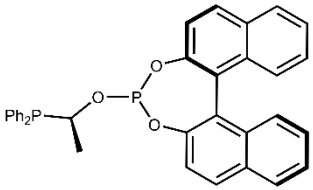

L8

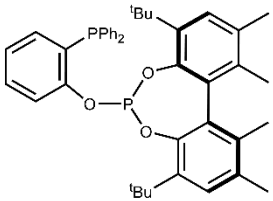

L9

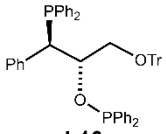

L10

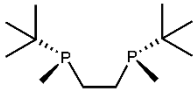

L11
(*S*,*S*)-*t*-Bu-BisP*

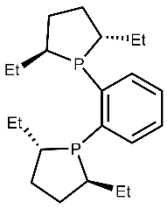

L12
(*S*, *S*)-Et-DUPHOS

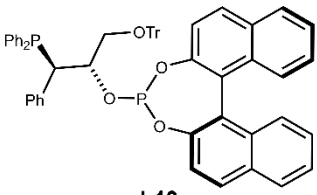

L13